Congress on Numerical Methods in Engineering 2011
Coimbra, 14 to 17 June, 2011

FLOW OF RED BLOOD CELLS THROUGH A MICROCHANNEL WITH A CONFLUENCE

Vladimir Leble[1*], Rui Lima[1,2], Carla S. Fernandes[1] and Ricardo P. Dias[1,2]

1: Escola Superior de Tecnologia e Gestão
Instituto Politécnico de Bragança
Campus de Santa Apolónia, Apartado 1134
5301-857 Bragança, Portugal
e-mail: wlodek29@gmail.com

2: CEFT - Centro de Estudos de Fenómenos de Transporte
Faculdade de Engenharia
Universidade do Porto
Praça Gomes Teixeira
4099-002 Porto, Portugal
e-mail: {ruimec, cveiga, ricardod}@ipb.pt

Keywords: Red blood cells, velocity profiles, confocal micro-PTV, confluence, microchannel

Abstract *Over the years micro-visualization techniques have been used to investigate in vitro blood flow through straight microchannels with dimensions close to in vivo capillaries. However, a few detailed studies have been performed in complex in vitro microvascular networks composed by diverging and converging bifurcations. The main purpose of present work is to show the application of a confocal micro-PTV system to track both flourescent particles and red blood cells (RBCs) through a rectangular polydimethysiloxane (PDMS) microchannel with a confluence. The measurements of the flow behaviour of trace particles suspended in pure water and RBCs in concentrated suspensions were performed in the surroundings of a confluence. After performing simulations with the commercial finite element software package POLYFLOW®, some experimental results were compared with the numerical ones. Experimental results for pure water were in a good agreement with numerical results. Overall, the RBCs velocities were higher than those for fluorescent particles which suggest that RBC deformability and cell-free layer formation around the apex of the confluence may play an important role on the observed deviations.*

1. INTRODUCTION

A microvascular network consists of short irregular vessel segments which are linked by numerous diverging and converging bifurcations. Although the phenomena of blood flow in microvascular networks have been studied for many years it still remains incompletely understood [1]. For instance, the blood flow behaviour in bifurcations is difficult to be analysed as it comprises the motion of extremely deformable cells in geometrically complex regions. It is therefore important to investigate in detail the behaviour of blood flow occurring at bifurcations in order to better understand the role of red blood cells in the process of delivering oxygen and materials to the organs and tissues.

The complexity to control and obtain detailed measurements of the blood flow behaviour through *in vivo* microvascular systems [2] has led to perform *in vitro* studies by using polydimethylsiloxane (PDMS) microchannels obtained by means of a soft-lithography technique [3-6]. In the present paper, by using a confocal micro-PTV system we investigated the variations in the velocity profile of both pure water and *in vitro* blood through a confluence (converging bifurcation). Moreover, the experimental data were compared numerically by using the commercial finite element software package POLYFLOW®. By using this combination we expect to gain understanding about several important parameters that affect the blood flow through a converging microvessel bifurcation.

2. EXPERIMENTAL SET-UP

The confocal micro-PTV system used in the present study consists of an inverted microscope (IX71, Olympus, Japan) combined with a confocal scanning unit (CSU22, Yokogawa, Japan) and a diode-pumped solid state (DPSS) laser (Laser Quantum Ltd, England) with an excitation wavelength of 532 nm and a high-speed camera (Phantom v7.1, U.S.A.). By using a soft-lithography technique we were able to manufacture a polydimethylsiloxane (PDMS) microchannel consisted with a bifurcation and confluence (see Figure 1). The PDMS microchannel was placed on the stage of the microscope where the flow rate of two working fluids was kept constant by means of a syringe pump (KD Scientific Inc., U.S.A.). The two working fluids used in this study were pure water and dextran 40 (Dx40) containing about 14% (14Hct) of human red blood cells (RBCs). The blood was collected from a healthy adult volunteer, where ethylenediaminetetraacetic acid (EDTA) was added to prevent coagulation. The RBCs were separated from the bulk blood by centrifugation and aspiration and then washed twice with physiological saline (PS). The washed RBCs were labelled with a fluorescent cell tracker (CM-Dil, C-7000, Molecular Probes) and then diluted with Dx40 to make up the required RBCs concentration by volume. All blood samples were stored hermetical at 4°C until the experiment was performed at controlled temperature of about 37°C. Detailed information about the experimental set-up, microchannel fabrication and RBC labelling used in the present study, has already been described previously [7-9].

3. MATERIALS AND METHODS

All the confocal images were recorded around the middle of the microchannels, using a piezo driver system and RT3D software from the Yokogawa Corporation. The series of x-y

confocal images were captured with a resolution of 640×480 pixels, at a rate of 100 frames/second with an exposure time of 9.4 ms. The recorded images were transferred to the computer and then evaluated in the image processing program ImageJ (NIH) [10] by using the manual tracking MtrackJ plugin [11] and automatic ParticleTracker 2D plugin [12] to detect and track particles in pure water and RBCs in Dx40 respectively.

Overall 13 videos of labelled RBCs flow were analysed, where each video consists of approximately 300 frames. Due to difference in videos quality, different settings for cell detection and linking were used in ParticleTracker plugin for each video. As during the experimental work the laser was illuminating the region of interest heterogeneously, some of RBCs has tendency to lose brightness for one or two frames. Therefore after evaluation, all tracks were checked manually to increase accuracy and remove incorrect detections and linking. Also, due to nonuniformity of laser illumination more tracks for lower part of the confluence were acquired (see Figure 4).

The density of fluorescent particles in pure water was higher comparing to labelled RBCs, hence manual MtrackJ plugin was used instead of automatic ParticleTracker. Because of close surrounding of neighbouring particles, different settings had to be used for each particle to track. Snap feature was always the same: bright centroid, however snap range varied between 7x7 and 13x13 px. The whole velocity filed obtained for pure water using described above technic is presented in Figure 3.

Afterwards Matlab script was implemented in order to obtain velocities fields shown in Figures 3-4. Both PTV fields and numerical results were put together into global system of coordinates using reference point which is a tip of an apex of the confluence. Another Matlab script was written to rotate fields simultaneously and produce velocity profiles in eleven selected planes described in Section 5.

The geometry displayed in Figure 1 was found from the visualization videos with visible walls of microchannels. Figure 2 shows the real geometry of the confluence and part of the geometry used in simulations.

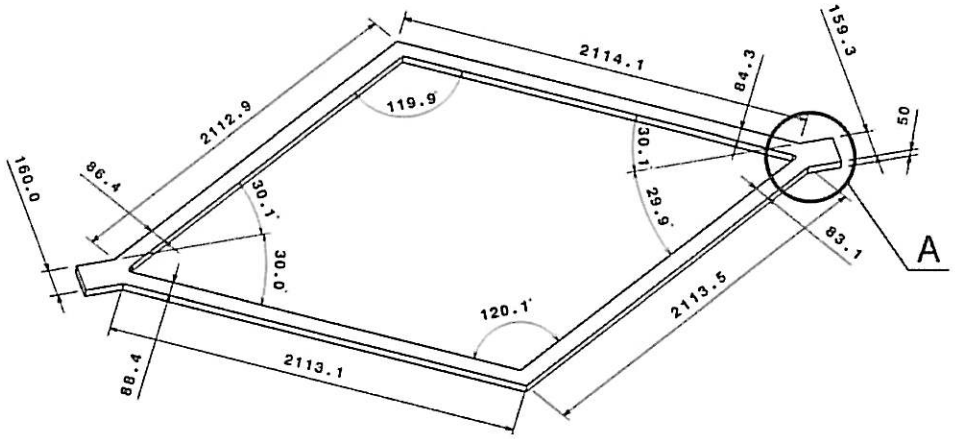

Figure 1. Full geometry of microchannels obtained from visualization videos. All dimensions are in micrometers.

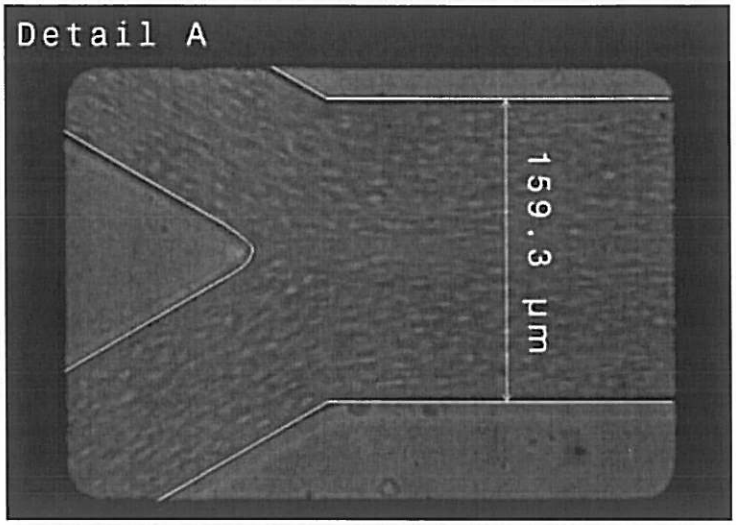

Figure 2. Detail A of Figure 1 showing the real geometry of the confluence and the geometry used in simulations.

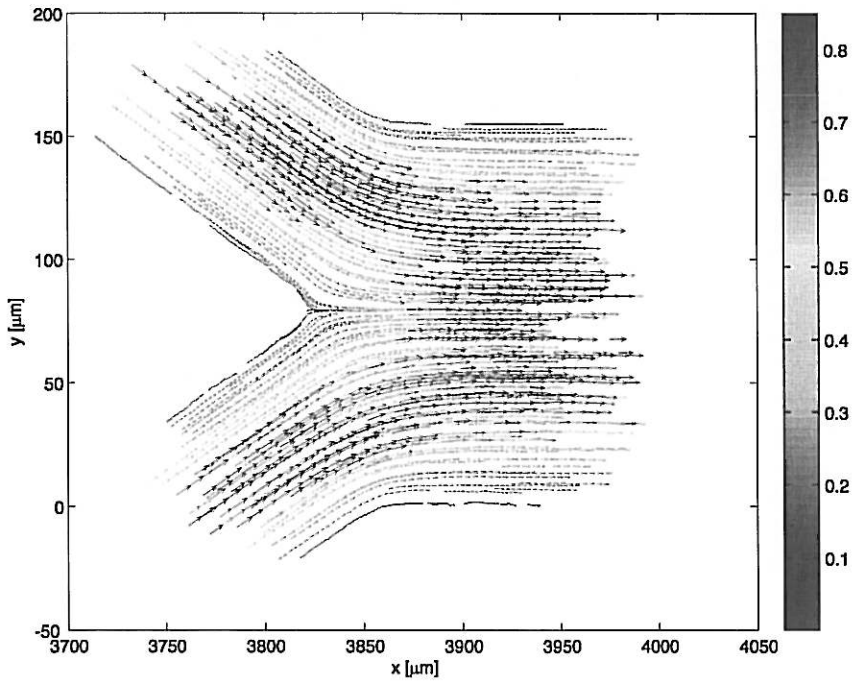

Figure 3. Velocity field obtained for water PTV.

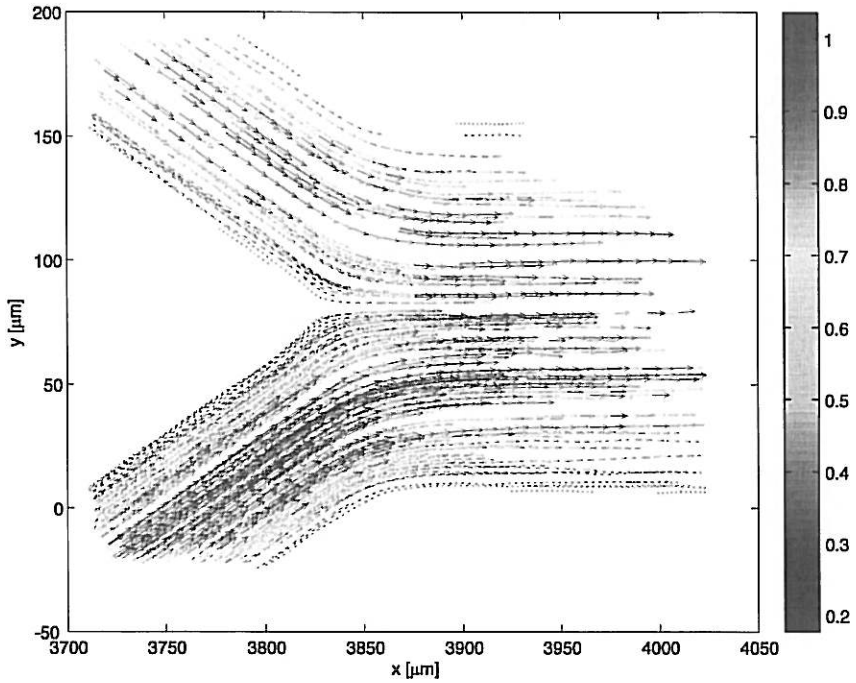

Figure 4. Velocity field obtained for red blood cells PTV

4. NUMERICAL SIMULATIONS

The numerical calculations for the laminar isothermal flow of blood were performed using the finite-element computational fluid dynamics (CFD) program POLYFLOW®. The simulations were carried out in a 3D geometry representing microchannels (see Figure 1) and the mesh used in the simulations was mainly constituted by quadrilateral elements (see Figure 5).

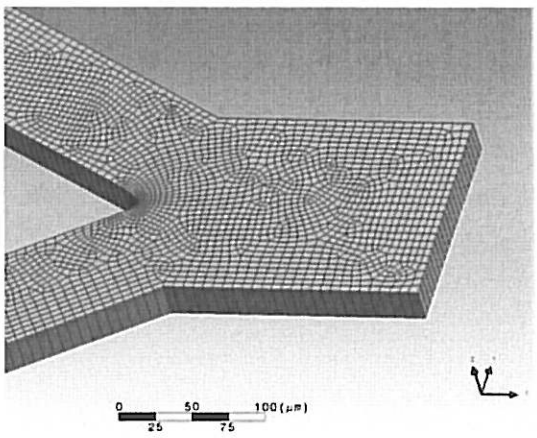

Figure 5. Mesh used in the simulations.

The equations solved were the conservation of mass and momentum equations for laminar incompressible flow of blood. The problem is a non-linear problem, so it was necessary to use an iterative method to solve the referred equations. In order to evaluate the convergence of this process, a test based on the relative error in the velocity field was performed. For the velocity field, the modification on each node between two consecutive iterations is compared to the value of the velocity at the current iteration. In the present work, the convergence value was set to 10^{-4}, since this value is appropriate for the studied problem [13-16].
The boundary conditions were established in order to reproduce the experimental conditions – a constant flow rate was imposed in the inlet of the microchannel – 3003.2 $\mu m^3/ms$ - and slip at the walls of the channel was assumed to be non-existent. In the numerical study, blood was considered as Newtonian and non-Newtonian fluid. In the latter case, the rheology of the blood was described by two different constitutive models - power law model and the Carreau model [17] – which are, respectively, expressed mathematically by the equations:

$$\eta = K\dot{\gamma}^{n-1} \tag{1}$$

$$\eta = \eta_\infty + (\eta_0 - \eta_\infty)\left[1 + (\lambda\dot{\gamma})^2\right]^{(n-1)/2} \tag{2}$$

where η is the viscosity of the fluid, K the consistency index, n the flow index behaviour, $\dot{\gamma}$ the shear rate, η_∞ the viscosity for high shear rates, η_0 the viscosity for low shear rates and λ is the natural time. For the blood, the rheological parameters present in the above equations are reported in Table 1.

Rheological model	η (Pa.s)	K (Pa.s^n)	n (-)	λ (s)	η_∞ (Pa.s)	η_0 (Pa.s)
Newtonian	0.00345	-	-	-	-	-
Power law model	-	0.035	0.6	-	-	-
Carreau model	-	-	0.3568	3.313	0.00345	0.056

Table 1. Rheological parameters of blood [17].

The numerical model designed for the present study – computational domain, mesh and boundary conditions - was validated by the comparison of the numerical and analytical velocity profiles for a fully developed flow in straight rectangular channel for a Newtonian fluid. The fully developed flow was obtained on length of 50μm from the entrance and in this region numerical and analytical solutions were compared and shown in Figure 6. Average difference between both solutions is 0.83%.

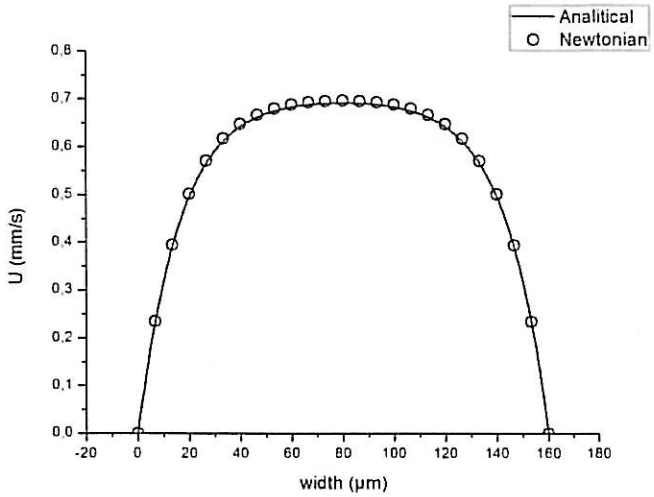

Figure 6. Comparison between simulation of Newtonian fluid and analitical solution for fully developed flow in straight, rectangular channel.

5. RESULTS AND DISCUTION

The velocity profiles were analysed in the regions shown in Figure 7. Figures from 9 to 11 show comparison between numerical simulation for water and PTV measurements for pure water and RBCs. Figure 8 displays the velocity field of RBCs superimposed onto the real geometry of the confluence.

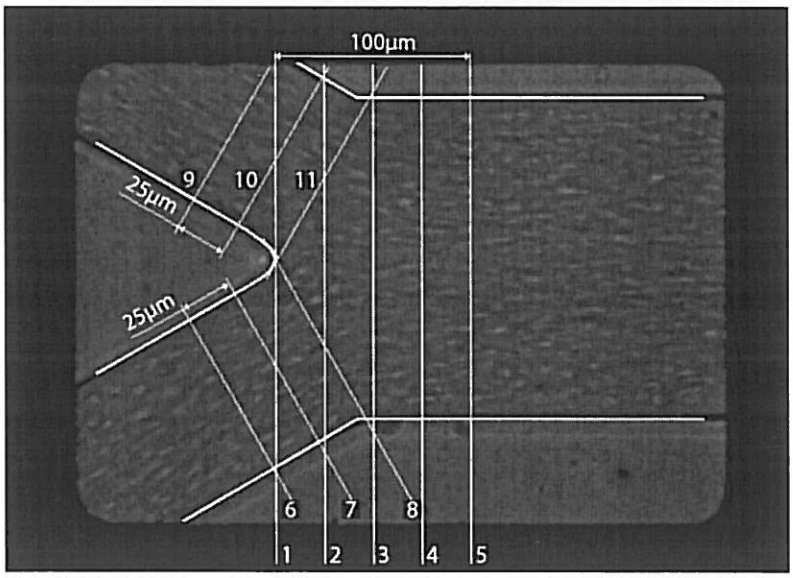

Figure 7. Real geometry and part of geometry used in simulations. Lines represent the planes where velocity profiles were collected and analyzed.

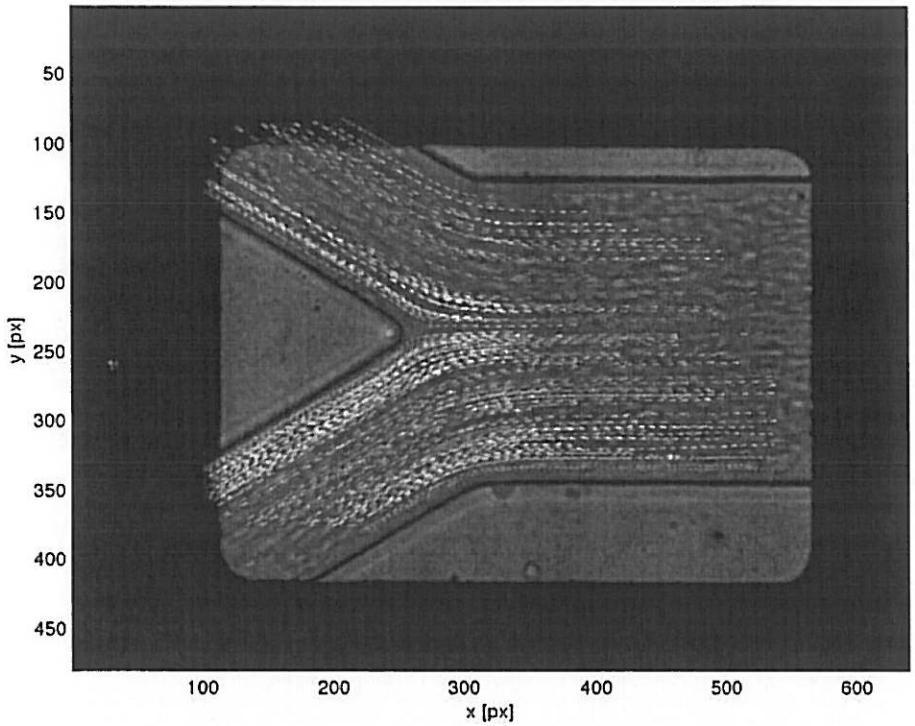

Figure 8. Real geometry of the confluence with overlaid velocity field of RBCs.

As displayed in Figure 9a, two streams enter the confluence and merge together producing two peaks in the velocity profile. Afterwards, along the straight rectangular channel, fully developed flow is progressively obtained. This trend is well shown by both - measurements and numerical results (see Figure 9). In referred figure it is possible to observe that the experimental results for water are in a good agreement with numerical simulations. Those measurements which are closer to the walls are more accurate, as fluorescent particles were moving slowly and during the exposure time they preserved rounded shape captured on the images, and therefore facilitated the localization of the particles centroid. In the central region of the channels, during the same exposure time, particles moved for a larger distance what resulted in elliptical shape captured on the videos. That, combined with irregular illumination, is the main reason for higher uncertainties and discrepancies between simulation and measurements away from the walls. However, general scattering around the numerical curves is clearly observed.

The same trend of accuracy happens to PTV measurements of RBCs. Despite some scattering of the collected data for RBCs, it can be clearly seen that in the central region the velocities of RBCs are higher than those obtained for pure water, see Figure 9(b-e). The cell-free layer created around the tip of the apex of the confluence can be seen in Figures 7 and 8. The existence of this cell-free layer explains the lack of RBCs in the centre of plane 1, see Figures 7 and 9a. It can be also observed that fluorescent particles in pure water can easily access this region.

Concerning Figure 10 (planes 6-8 in Figure 7), an important note has to be made, i.e., the right side of the graphs represents regions closer to the apex of the confluence, while the left side represents regions closer to the external wall of the whole geometry. The opposite happens for Figure 11 (planes 9-11 in Figure 7), where the left side of the graphs represents regions closer the apex and the right side regions closer to the external wall. In Figure 10 we can see that velocities of the RBCs are in a better agreement with the fluorescent particles velocities in the regions closer to the external wall. In the centre and close to the apex the RBCs velocities are higher than those obtained for pure water. These results are in accordance with the results displayed in Figures 11 and 9a. This phenomenon may be explained not only by the high deformability of the RBCs, but also by the existence of a pronounced cell-free layer in the vicinity of the tip of the apex and in the region after it. In this region there is a decrease in the local haematocrit (Hct), and as a result the RBCs, which are much more deformable than the rigid trace particles, tend to flow with higher velocities than those of fluorescent particles in pure water. In Figure 7 we may see that the cell-free layer is propagated in a straight, horizontal line coming out of the tip of the apex. Moreover, it can be also observed that the local Hct nearby the referred line is lower in comparison to the regions closer to the external walls. Therefore, the velocities of RBCs obtained in the central region of the confluence (see Figure 9) are also higher, than those of particles in pure water.

As expected [18], the results obtained from simulation of blood as a homogeneous, non-Newtonian fluid do not describe the higher velocities of RBCs. For instance, in a plane after the confluence (see Figure 12) we may see that the numerical velocities in the central region of the channel, obtained with different non-Newtonian models, are below the velocities obtained by Newtonian fluid model.

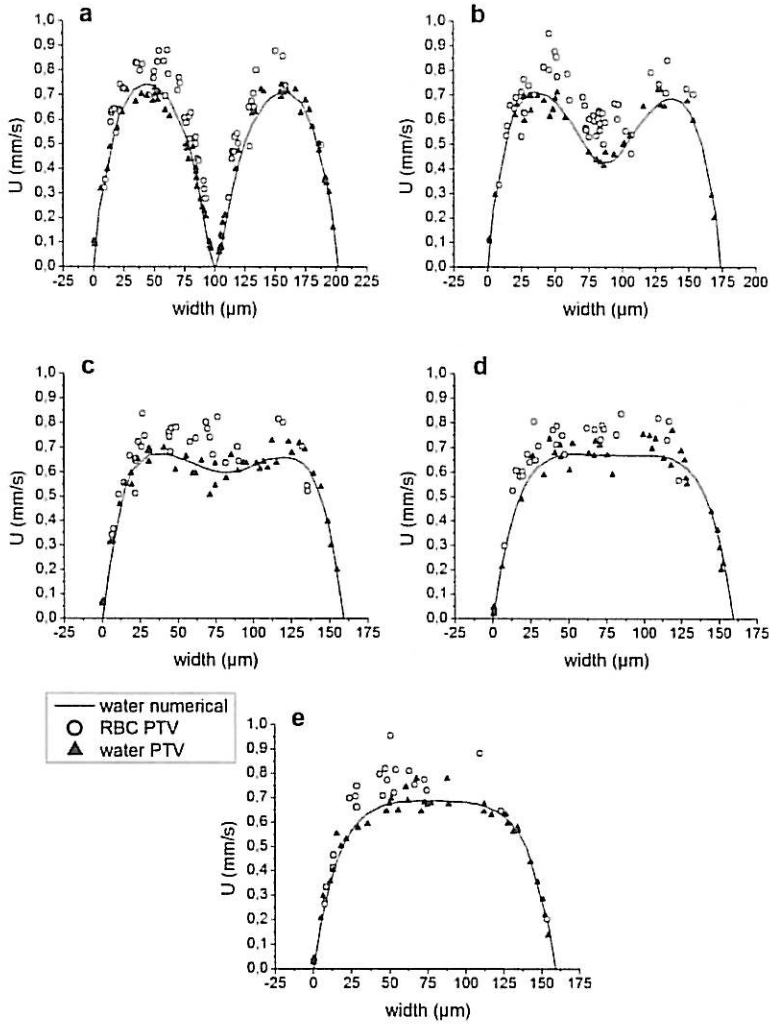

Figure 9. Velocity profiles for both computational and experimental results after confluence in regions 1-5 (a-e, respectively).

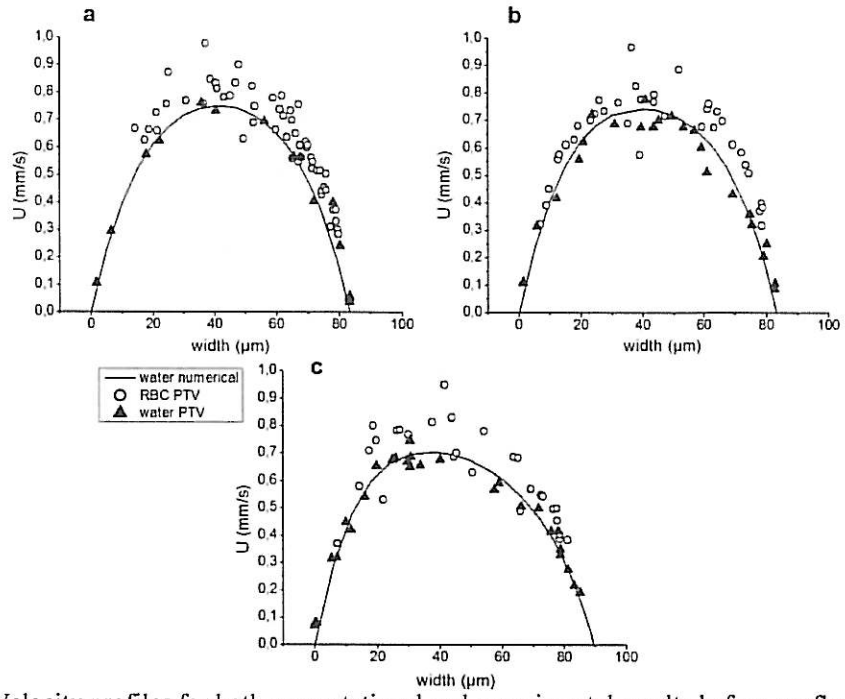

Figure 10. Velocity profiles for both computational and experimental results before confluence in regions 6-8 (a-c, respectively).

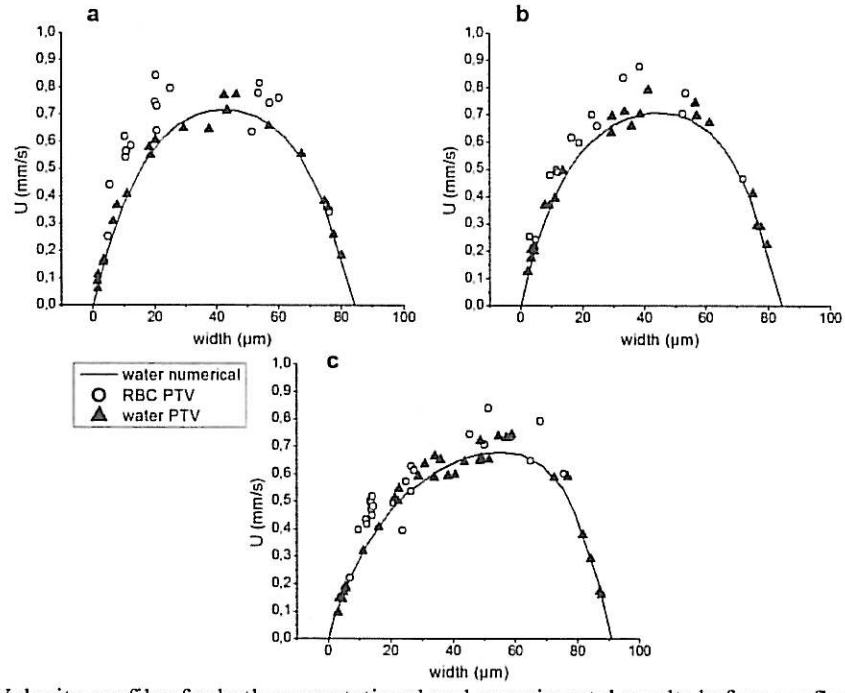

Figure 11. Velocity profiles for both computational and experimental results before confluence in regions 9-11 (a-c, respectively).

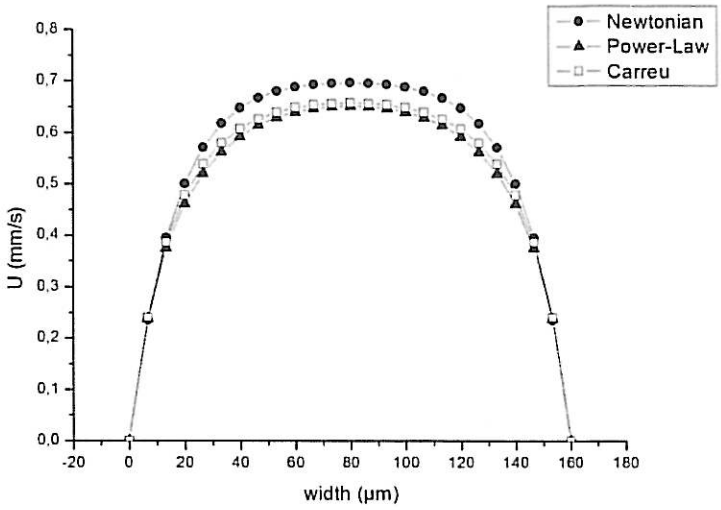

Figure 12. Comparison between different computational models.

6. CONCLUSIONS

The simulations performed with a finite-element computational fluid dynamics (CFD) program POLYFLOW emphasized the need of development of a multiphase approach. PTV results acquired for pure water were in a good agreement with numerical results. PTV results obtained for RBCs in parent vessels and daughter vessel were higher than those for fluorescent particles in some regions. In the former case this occurs close to the apex, while in the latter case that effect was observed after the apex, in the central region of the channel. The RBC deformability and the existence of the cell-free layer in the vicinity of the apex and after the apex may explain this behaviour. Concerning the daughter vessel, in future works we will study the behaviour of RBCs velocity in regions more distant from the apex than those analysed in the present work. This may help to clarify the influence of the cell-free layer on RBCs velocity.

ACKNOWLEDGEMENTS

The authors acknowledge the financial support provided by: PTDC/SAU-BEB/108728/2008, PTDC/SAU-BEB/105650/2008 and PTDC/EME-MFE/099109/2008 from the FCT (Science and Technology Foundation) and COMPETE, Portugal.

REFERENCES

[1] Popel, A., Johnson, P., Microcirculation and Hemorheology. Annu. Rev. Fluid Mech. 37: 43–69, 2005.

[2] Nakano, A., Sugii, Y., et al.; Velocity Profiles of Pulsatile Blood Flow in Arterioles with Bifurcation and Confluence in Rat Mesnetery Measured by Particle Image Velocimetry. JSME Interantional Journal, Serie C, 4, 48, 444–452, 2005.

[3] Shevkoplyas S. S:, Yoshida T., Munn L. L., Bitensky M. W., 2005. Biomimetic Autoseparation of Leukocytes from Whole Blood in a Microfluidic Device. Anal. Chem., 77, 933-937, 2005.

[4] Shevkoplyas S. S:, Yoshida T., Gifford S. C., Bitensky M. W., 2006. Direct measurement of the impact of impaired erythrocyte deformability on microvascular network perfusion in a microfluidic device. Lab Chip, 6, 914–920, 2006.

[5] Lima, R., Wada, S., et al., "In vitro blood flow in a rectangular PDMS microchannel: experimental observations using a confocal micro-PIV system". Biomedical Microdevices, 2, 10, 153-67, 2008.

[6] Lima, R., Fernandes C.S., et al., "Microscale flow dynamics of red blood cells in microchannels: an experimental and numerical analysis", In: Tavares and Jorge (Eds), Computational Vision and Medical Image Processing: Recent Trends, Springer, Vol.19, 297-309, 2011.

[7] Lima, R., Wada, S., et al., "In vitro blood flow in a rectangular PDMS microchannel: experimental observations using a confocal micro-PIV system". Biomedical Microdevices, 2, 10, 153-67, 2008.

[8] Lima, R., Ishikawa, T., et al., "Measurement of individual red blood cell motions under high hematocrit conditions using a confocal micro-PTV system,", Annals of Biomedical Engineering, 37, 8, 1546-1559, 2009.

[9] Lima, R., Fernandes C.S., et al., "Microscale flow dynamics of red blood cells in microchannels: an experimental and numerical analysis", In: Tavares and Jorge (Eds), Computational Vision and Medical Image Processing: Recent Trends, Springer, Vol.19, 297-309, 2011.

[10] Abramoff, M.D., Magelhaes, P.J., Ram, S.J. "Image Processing with ImageJ". Biophotonics International, volume 11, issue 7, pp. 36-42, 2004.

[11] Meijering, E., Smal, I., and Danuser, G., Tracking in Molecular Bioimaging. IEEE Signal Processing Magazine 3 (23): 46-53, 2006

[12] I. F. Sbalzarini and P. Koumoutsakos. Feature Point Tracking and Trajectory Analysis for Video Imaging in Cell Biology, Journal of Structural Biology 151(2):182-195, 2005

[13] R.P. Dias, C.S. Fernandes, et al., "Starch analysis using hydrodynamic chromatography with a mixed-bed particle column", *Carbohydrate Polymers* Vol. **74**, pp. 852-857, (2008)

[14] C.S. Fernandes, R.P. Dias, et al., "Simulation of stirred yoghurt processing in plate heat exchangers", *Journal of Food Engineering* Vol. **69**, pp.281-290, (2005)

[15] C.S. Fernandes, R.P. Dias, et al., "Laminar flow in chevron-type plate heat exchangers: CFD analysis of tortuosity, shape factor and friction factor", *Chemical Engineering and Processing: Process Intensification* Vol. **46**, pp. 825-833, (2007)

[16] C.S. Fernandes, R.P. Dias, et al., "Friction factors of power-law fluids in plate heat exchangers", *Journal of Food Engineering* Vol. **89**, pp. 441-447, (2008)

[17] B.M. Johnston, P.R. Johnston, et al., "Non-Newtonian blood flow in human right coronary arteries: steady state simulations", *Journal of Biomechanics* Vol. **37**, pp. 709-720, (2004)

[18] W.L. Wilkinson, *Non-Newtonian Fluids: Fluid Mechanics, Mixing and Heat Transfer,* Pergamon Press, 1960.